J Soils Sediments (2013) 13:1579–1588
DOI 10.1007/s11368-013-0746-7

SOILS, SEC 3 • REMEDIATION AND MANAGEMENT OF CONTAMINATED OR DEGRADED LANDS • RESEARCH ARTICLE

Interactions between cations and water molecule bridges in soil organic matter

Gabriele E. Schaumann · Daniela Gildemeister · Yamuna Kunhi Mouvenchery · Sandra Spielvogel · Dörte Diehl

Received: 2 February 2013 / Accepted: 21 June 2013 / Published online: 10 July 2013
© Springer-Verlag Berlin Heidelberg 2013

Abstract
Purpose Nutrient release, soil wettability, water binding, and matrix rigidity of soil organic matter (SOM) can be affected by cross-links between segments of SOM, cations, and water molecule bridges (WaMB). Not all cation effects on SOM can be explained with the currently accepted idea that multivalent cations cross-link organic matter segments via direct cation bridges (CaB). The objective was to understand these interactions and their effect on SOM matrix rigidity and wettability.
Materials and methods We modified cation composition of two peats and an organic surface layer (OSL) using cation exchange resin to remove cations and solutions of Na^{+}, Ca^{2+}, or Al^{3+} to enrich samples with cations. SOM matrix rigidity was determined at 4 and >8 weeks after treatment via the WaMB transition temperature T^*, using differential scanning calorimetry. Wettability was measured via sessile drop contact angle (CA).
Results and discussion The effect of cation removal on T^* depended on cation exchange capacity and initial cation content. Cation addition to OSL increased T^*. This effect increased with increasing cation loading and valency, and T^* correlated with CA. Classical cross-linking can neither explain the higher heterogeneous matrix of Ca-treated than Al-treated samples nor the aging-induced convergence of T^* for different cations and concentrations. The latter is likely due to interaction between CaB and WaMB in SOM.
Conclusions Associations of CaB and WaMB evolve slowly and form a supramolecular network in SOM. Those dynamic associations can fix molecular arrangements inducing water repellency and increase kinetic barriers for the release and uptake of water and nutrients from aged soil.

Keywords Cross-links · Differential scanning calorimetry · Matrix rigidity · Multivalent cation · Soil organic matter · Water molecule bridges (WaMB) · Water repellency

Responsible editor: Jianming Xu

G. E. Schaumann (✉) · D. Gildemeister · Y. Kunhi Mouvenchery · S. Spielvogel · D. Diehl
Institute for Environmental Sciences, Department of Environmental and Soil Chemistry, University Koblenz-Landau, Fortstr. 7, 76829 Landau, Germany
e-mail: schaumann@uni-landau.de

Present Address:
S. Spielvogel
Institute of Integrated Natural Sciences, University Koblenz-Landau, Universitätsstr. 1, 56070 Koblenz, Germany

1 Introduction

Controlling chemical activity and release rates, solid soil organic matter (SOM) plays a central role for soil wettability and for availability of nutrients, water, and organic chemicals (Doerr et al. 2000; Pignatello 2012). Release and degradation of compounds can be controlled by physical entrapment in soil aggregates (Virto et al. 2011), molecular aggregates of humic substances (Li et al. 2013), or by kinetic barriers in the solid SOM matrix (Schaumann et al. 2000; Schaumann 2006). Rigid matrixes generally slow down transport of ions and molecules (Suvorova et al. 1999), e.g., glassy phases in natural organic matter (NOM) are made responsible for sequestration, sorption hysteresis, and increased desorption resistance of organic chemicals (LeBoeuf and Weber 2000a; Schaumann 2006). They can be softened by changes in temperature or moisture (LeBoeuf and Weber 2000a; Schaumann 2006), which can suddenly increase kinetic availability of any compound. Knowledge of the partly unknown mechanisms modifying matrix rigidity is essential for a profound understanding and prediction of pollutant and nutrient retention in soil (Schaumann and Bertmer 2008).

Up to now, two mechanisms of matrix softening have been demonstrated for NOM. Classical glass transitions (LeBoeuf and Weber 2000b) are induced by heating above the glass transition temperature, T_g, in natural and model humic

substances (LeBoeuf and Weber 2000b). Glass transitions are reversible transformations in amorphous regions between a hard and brittle state and a rubbery state (Seyler 1994). More relevant in SOM are water molecule bridge (WaMB) transitions, which are induced by the disruption of WaMB between molecular segments of SOM (Hurrass and Schaumann 2005; Schaumann and LeBoeuf 2005; Schaumann and Bertmer 2008; Aquino et al. 2009). WaMB resemble small water clusters pinned up between two functional groups and reduce mobility of molecular segments (Aquino et al. 2009). WaMB transitions are induced by heating above the WaMB transition temperature (T^*) (Hurrass and Schaumann 2005; Schaumann and LeBoeuf 2005) or by changes in moisture conditions (Schaumann 2005; Schaumann and LeBoeuf 2005; Hurraß and Schaumann 2007). T^* characterizes thermal stability of WaMB, which determines matrix rigidity in their surroundings (Schaumann and LeBoeuf 2005; Schaumann and Thiele-Bruhn 2011). Matrixes stiffened by WaMB undergo slow physicochemical aging, in which redistribution of water molecules increases the number and strength of WaMB and thus T^* (Schaumann 2005; Hurraß and Schaumann 2007; Schaumann and Bertmer 2008). WaMB transitions in SOM have been observed and quantified by differential scanning calorimetry (DSC) and thermomechanical analysis (Schaumann et al. 2005; Schaumann and LeBoeuf 2005; Hurraß and Schaumann 2007) and demonstrated by ^{1}H NMR wideline spectroscopy (Schaumann and Bertmer 2008; Jaeger et al. 2011). Exploring the currently available literature on WaMB transitions shows that up to now, the only available method to quantify T^* is DSC.

Coordinative cross-links of molecular segments of organic matter (OM) via cation bridges (CaB) can also increase matrix rigidity (Lewis and Miller 1993). CaB have been suggested to explain cation effects on aggregate stability (Gaiffe et al. 1984), stability of SOM against degradation (Scheel et al. 2008), deceleration of release of dissolved organic carbon (DOC) in the presence of Ca^{2+} (Schaumann 2000), and increased mobilization of NOM in the presence of chelating agents (Yang et al. 2001). They can generate supramolecular associations of NOM molecules in aqueous environments (Piccolo 2002; Simpson et al. 2002; Wershaw 2004) and reduce molecular mobility in humic acids (HA) (Nebbioso and Piccolo 2009). Furthermore, aggregation of humic acid upon cation addition was found to be very sensitive to pH and the cation concentration (Tan et al. 2009). CaB were further used to explain sorption anomalies of organic chemicals in HA (Yuan and Xing 2001; Lu and Pignatello 2004) and SOM (Yang et al. 2001).

If CaB increase matrix rigidity, they can also alter SOM surface properties, as they can fix orientation of hydrophilic OM groups towards the cations in the interior, leading to partial charge compensation (Tan et al. 2011) and leaving the hydrophobic parts at the surface. Reorientation of the hydrophilic groups upon contact with water (Doerr et al. 2007; Diehl et al. 2010) would then be impeded by CaB with the consequence of increased wetting resistance.

The nature of CaB in SOM is not fully understood (Kunhi Mouvenchery et al. 2012). Cross-linking via direct CaB requires that functional groups are close enough to interact with one cation (Kunhi Mouvenchery et al. 2012). In SOM, not all functional groups fulfill this prerequisite. Larger distances could be bridged by a combination of CaB and WaMB (Aquino et al. 2011; Schaumann and Thiele-Bruhn 2011; Schaumann et al. 2013). The relevance of direct CaB, WaMB, and their interactions for matrix rigidity is unknown. Involvement of WaMB in CaB is highly relevant as it will lead to higher dynamics than direct CaB and may even overbalance individual cation effects. It is, therefore, essential to know to which extent classical cross-links, WaMB and CaB control matrix rigidity, and surface properties and how they interact with each other.

The objective of our study was to understand the role of WaMB in cation–SOM interactions and their effect on matrix and surface properties of SOM. In this first study, we exemplarily investigated the organic layer of a Haplic Podzol and two peat samples in interaction with Na^+, Ca^{2+}, and Al^{3+}. Transfer to further soils and more cations requires additional studies. Ca^{2+} and Al^{3+} are known for their cross-linking characteristics, are typically present in soils with high SOM content like Podzols or Rendzinas, and we expect differences in their cross-linking efficiency due to their different valency. We tested the following hypotheses for cation effects: (1) Multivalent cations form cross-links between OM molecule segments and increase matrix rigidity. This increase is stronger for higher cation valency and for higher cation concentration (classical cross-linking), (2) cation-treated SOM reveals WaMB transitions with all typical characteristics including restricted reversibility and physicochemical aging, (3) the effect of WaMB overbalances the effect of CaB, and (4) CaB block reorientation of hydrophilic functional groups towards the surface of SOM and thus increase water repellency.

2 Material and methods

2.1 Samples, sample preparation, and soil analysis

We used two Histosols and a sample from an organic surface layer (OSL) of a Haplic Podzol. The OSL was sampled in a forest stand dominated by 80-year-old Norway spruces (*Picea abies* L. [Karst.]) in Southern Germany (thickness 0.15 m). The Histosol samples were taken from a Sapric Histosol from "Totes Moor" near Hannover (Jaeger et al. 2010) (peat 1; sampling depth 1.0–1.1 m) and from a Eutric Histosol from Heudorfer Ried, a meliorated fen in southwest Germany (Schneckenburger et al. 2012) (peat 2; sampling depth 0.0–0.2 m). The peat

samples were air dried prior to use. OSL samples were shock frozen and stored at −18 °C. Shortly before experiments, the OSL samples were gently unfrozen in a fridge, air dried, and sieved to ≤1 mm. The effective cation exchange capacity (CEC_{eff}) was determined using barium chloride according to DIN ISO 11260 and DIN ISO 13536 (Gustafsson et al. 2003). pH was measured in 0.01 M $CaCl_2$ at a soil/solution ratio of 1:2.5. Basic characteristics of the samples are summarized in Table 1.

2.2 Removal of cations via cation exchange resin treatment

In order to analyze the effect of cations naturally present in the samples, they were treated with cation exchange resin in order to extract large part of exchangeable cations (Kaupenjohann and Wilcke 1995; Lang and Kaupenjohann 2004). For the peats, one sample was extracted, and for the OSL, experiments were conducted in duplicates. Demineralization experiments were conducted with an acidic cation exchange resin (ion resin Amberlite® IR120, H^+-Form, exchange capacity 2.3 $mmol_c g^{-1}$, Merck, Darmstadt). Of the resin, 2.5 g was packed in a polypropylene net (mesh size 72 μm). Each resin bag was washed in 10% HNO_3 for 30 min and rinsed with deionized water to remove DOC and free acid prior to use.

Two grams of sample and 50 ml of water were mixed for 15 min in a horizontal shaker to assure complete wetting. Resin bags were added and the suspension was treated in a horizontal shaker for 24 h. pH was monitored after 30 min and after 24 h. In contrast to Kaupenjohann and Wilcke (1995), pH adjustment was not necessary as it was close to the required pH 3. After 24 h, the resin bag was removed and rinsed with deionized water. The suspension was filtered (0.45 μm cellulose nitrate filters, Sartorius®) for DOC measurements. In order to extract the cations removed from the soil, resin bags were extracted in 50 ml HNO_3 for 2 h. Extracts were analyzed for Ca^{2+} and Mg^{2+} via AAS (PerkinElmer 4100). Samples were stored for 4 weeks (Section 2.4) prior to DSC measurement.

Table 1 Basic properties of the three samples used for the batch experiments in this study (arithmetic means and standard deviations of values acquired from three to seven replicates per measurement)

	Organic surface layer from Haplic Podzol (South Germany)	Peat 1 Sapric Histosol (Fuhrberg)	Peat 2 Eutric Histosol (Heudorfer Ried)
pH	3.7±0.1	2.7±0.1	5.8±0.1
SOC, mg g^{-1}	430±40	539±30	250±25
CEC_{eff}, $mmol_c kg^{-1}$ soil	303±20	123±12	680±70
CEC_{eff}, $mmol_c kg^{-1}$ OC	705±120	228±35	2,720±540
Ca^{2+}, $mmol_c kg^{-1}$	165±10	45±1	944±20
Mg^{2+}, $mmol_c kg^{-1}$	43±5	22±1	480±48
Al^{3+}, $mmol_c$ kg^{-1}	60±3	11±3	286±10

2.3 Batch experiments for cation addition

Cation (Ca^{2+}, Al^{3+}, and Na^+) addition experiments were conducted with the OSL sample. The peat samples had to be excluded due to reasons discussed as a first result of this study in Section 3. Ten grams of OSL was treated at pH 4 with 250 ml solutions of calcium nitrate, aluminum nitrate, and sodium nitrate. At this pH, Al^{3+} occurs as hydrated cation and hydroxide precipitates are not expected (Johnson 2002; Nierop et al. 2002). Seven different concentrations were prepared for Ca^{2+} (1, 2, 4, 8, 10, 16, and 20 $mmol_c l^{-1}$) and for Al^{3+} (0.15, 0.75, 1.5, 6, 12, 18, and 24 $mmol_c l^{-1}$) and three different concentrations for Na^+ (10, 50, and 100 $mmol_c l^{-1}$). In preliminary experiments, these concentrations gave the best distribution between the original cation content and CEC_{eff}. Samples were prepared at least in duplicates. Suspensions were shaken for 3 h in a horizontal shaker. pH was monitored after 0.5 and 1.5 h and adjusted with 1 M HNO_3 or 0.5 M NaOH to pH 4, if necessary. Then, the suspensions were filtered (589/2 ashless filter papers, Whatman). A subsample was treated in batch with deionized water as described above, to obtain a control sample without salt addition (named "control").

2.4 Sample storage and physicochemical aging

After batch experiments, all samples were dried for 4 days at 25 °C in an oven and stored at 20 °C and 76% relative humidity (RH) over saturated sodium chloride solution in a desiccator. Aging effects were studied by DSC in all samples following isothermal storage at 20 °C and 76% RH for at least 8 weeks.

2.5 Chemical analysis of treated samples

To quantify the total amount of cations in the treated soil samples, two aliquots of each sample (1.5 g) were extracted with 40 ml 0.025 M ammonium ethylenediaminetetraacetate solution (99%, p.a., Carl Roth GmbH) at pH 4.6 for 3 h, followed by extraction using 1 M ammonium tetra acetate solution (10 min). The resulting extracts were analyzed for Ca^{2+}, Al^{3+}, Mg^{2+}, Fe^{3+}, and Mn^{2+} concentrations. Ca^{2+} and Mg^{2+} in extracts and supernatants were analyzed using flame AAS (PerkinElmer 4100), Fe^{3+} and Mn^{2+} were analyzed using graphite tube AAS (PerkinElmer 4100), and Al^{3+} was analyzed using a Varian AAS (AA 240 FS, N_2O/acetylene flame). In addition, we analyzed the supernatants of all batch experiments (Section 2.3) to evaluate the removal of cations and dissolved organic matter (DOM) from the sample. Supernatants were analyzed for pH, Al^{3+}, and Ca^{2+} and selected supernatants were additionally analyzed for Mg^{2+}, Fe^{3+}, and Mn^{2+}, as described above. DOC was

determined after filtration (0.45 μm Sartorius® cellulose nitrate filters pre-flushed with warm deionized water) using a TOC Analyzer Multi C/N 2100 (Analytik Jena) after acidification and outgassing of inorganic carbon.

2.6 Differential scanning calorimetry

DSC experiments were performed in order to quantify T^* (Schaumann 2005; Schaumann and LeBoeuf 2005) with a DSC Q1000 (TA Instruments, Germany) using a refrigerated cooling system and nitrogen as purge gas. One- to three-milligram samples were placed in aluminum pans, which were hermetically sealed. Three to seven replicates per sample were measured depending on the thermogram quality. The temperature program involved abrupt cooling to −50 °C, heating with 10 K min^{-1} from −50 to 110 °C, followed by a second abrupt cooling and subsequent heating cycle. Baseline was corrected with the TZero technology® by TA Instruments. Data were analyzed using Universal Analysis 4.1 (TA Instruments).

DSC thermograms were checked for step transitions and for their reoccurrence in a second heating run. Step transitions occurring only in the first heating run were interpreted as WaMB transitions (Schaumann and LeBoeuf 2005). T^* is indicated by the inflection point, which was determined by the application of three tangent lines, and the change of heat capacity (ΔC_p) was calculated from the height of the central tangent line.

2.7 Sessile drop contact angle

The sessile drop CA was determined according to Diehl and Schaumann (2007). The sample was fixed on a glass slide (76×26×1 mm, Roth, Germany). Therefore, one side of the slide was covered by a double-sided adhesive tape (tesafix® 4934, tesa, Germany) and loaded with a layer of sample grains which was slightly pressed onto the tape with a spatula. Excess sample material was removed by carefully knocking the glass slide. The loading and removal of excess material was repeated three times to obtain a closed coverage by a one grain layer. At 20 °C, three to six drops of 100 μL demineralized water were placed on the sample layer. Drop shape was recorded from a side view of the drops by a digital camera (PowerShot A 300, Canon, Japan) posed exactly at the height of the sample layer. CA was determined after a contact time of 1 min fitting an ellipse to the drop contour, a baseline to the sample surface, and calculating the CA using the software SCA 20 (V3.10.7) from Dataphysics (Filderstadt, Germany).

2.8 Statistical analysis

Statistical analysis was performed using the software Origin 7.5 (OriginLab Corporation). Where linear trends were tested, we used linear regression. The probability given in the respective figures corresponds to that of the hypothesis that the slope is 0. Box plots of datasets of T^* display their 25 and 75% percentile, their average, and their median. Differences between datasets were analyzed using one-way ANOVA.

3 Results and discussion

3.1 Soil properties

The OSL sample was acidic (pH 3.7) with CEC_{eff} of 303 $mmol_c kg^{-1}$ and contained 430 mg g^{-1} organic carbon (see Table 1). Peat 1 was more acidic (pH 2.7), contained considerably more organic carbon (539 mg g^{-1}), but had a lower CEC_{eff} (123 $mmol_c kg^{-1}$), while peat 2 revealed low acidity (pH 5.8), contained less organic carbon (250 mg g^{-1}), and had the highest CEC_{eff} (680 $mmol_c kg^{-1}$). The samples thus span a wide range of acidity, CEC_{eff}, and OM content and, therefore, likely contain OM differing in quality.

3.2 DSC thermograms

Representative DSC thermograms are shown in Fig. 1 for the OSL. The thermograms of the first heating cycle showed a step between 56 and 64 °C with ΔC_p of 0.1-0.3 J g^{-1} K^{-1}. The step disappeared in the second cycle and was thus interpreted as WaMB transition. T^* was similar to that for samples of other peats and OSLs (Schaumann and LeBoeuf 2005; Schaumann et al. 2005).

Thermograms of peat 1 were more complex than those of peat 2 and OSL, consisting of an overlap of two processes in the same temperature region (data not shown), the nature of which is currently under investigation. One of these processes is non-reversing and fulfills the prerequisites for a WaMB

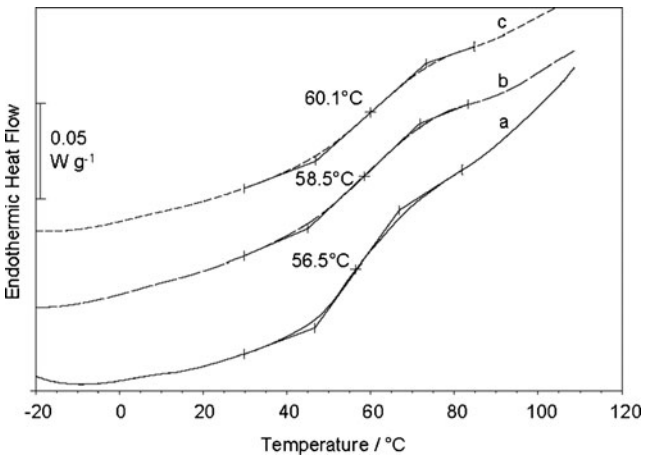

Fig. 1 Representative DSC thermograms of the first heating cycle of the OSL ample treated with calcium. **a** Reference sample only moistened (Ca^{2+} content=160 $mmol_c kg^{-1}$). **b** Ca-treated sample (Ca^{2+} content=175-$mmol_c kg^{-1}$). **c** Ca-treated sample (Ca^{2+} content=220 $mmol_c kg^{-1}$)

transition. Due to the overlap, determination of T^* leads for peat 1 to an uncertainty (ΔT^*) of ±1 °C.

3.3 Effects of cation removal

Table 2 shows the effects of the resin treatment on the removal of cations with respect to the untreated samples. Ninety to 100% of Mg and Ca was removed from all soil samples. In peat 2, exchangeable Ca and Mg and their removal considerably exceeded the CEC_{eff}. Part of the Ca might have been present as soluble salts, or part of the Ca and Mg could have occupied single functional groups, with the consequence of local charge reversal neutralized by negatively charged counter ions. The idea that cation charge is not completely neutralized by functional groups in peat 2 is further supported by the strong pH decrease from 6.2 to 2.6 during resin treatment, corresponding to an increase in H^+ concentration by a factor of 242. pH remains constant only if H^+ released from the exchange resin can bind to exchange sites formerly occupied by cations (Lang and Kaupenjohann 2004).

In peat 1 and OSL, H^+ concentration increased only by a factor of 15 (pH 4.0→2.8) and 45 (pH 4.4→2.8), respectively, and the amount of released cations did not exceed CEC_{eff}. Thus, large parts of the released cations were bound to two functional groups of OM in these samples.

Also, the effect of cation removal on T^* differed between the samples (Fig. 2). While T^* decreased for OSL and peat 1 by 2.5 and 1.5 °C, respectively, an increase by nearly 3 °C was observed for peat 2. Thus, removal of multivalent cations can either increase or decrease matrix rigidity, depending on the soil sample. The unexpected T^* increase in peat 2 coincides with its initial cation supersaturation.

Thus, high Ca^{2+} contents destabilize the supramolecular OM matrix structure, while intermediate and low Ca^{2+} contents stabilize it. The T^* cation content relation may thus have a maximum at a cation content indicating optimal cross-linking. In this view, the stronger decrease of T^* upon demineralization of OSL than of peat 1 suggests that OSL was initially closer at its rigidity maximum. Alternatively, cross-linking potential in peat 1 could be lower than in OSL due its low CEC_{eff}.

Table 2 Changes in soil organic carbon (ΔSOC) content, in exchangeable Ca^{2+} and Mg^{2+} (ΔCa, ΔMg) and in pH (H_2O) due to treatment with cation exchange resin. pH after treatment refers to the final pH (24 h)

	ΔSOC, g kg^{-1}	ΔCa, $mmol_c kg^{-1}$	ΔMg, $mmol_c kg^{-1}$	pH (H_2O) before treatment	pH (H_2O) after treatment
Peat 1	1.2	40	20	4.0	2.8
Peat 2	8.4	960	26	6.2	2.6
OSL	2.5	160	38	4.4	2.8

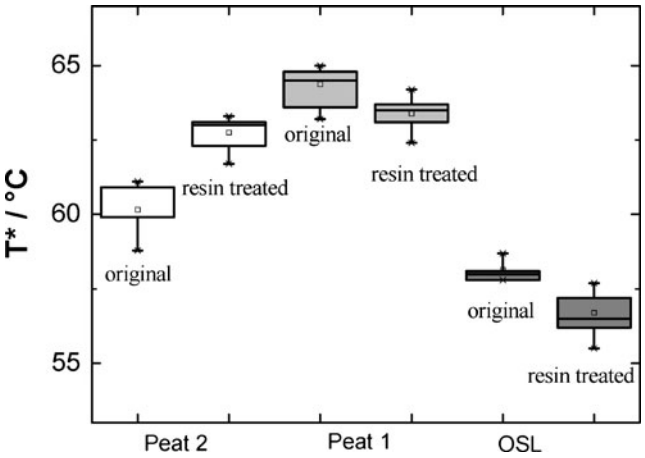

Fig. 2 WaMB transition temperature, T^*, before and after treatment of the three samples with cation exchange resin. The *box plots* refer to results of at least six independent measurements per sample

Choice of samples for the cation addition approach In the cation-overloaded peat 2, further cation addition will not change the OM cation saturation. Therefore, it was excluded from following experiments. As changes in T^* of peat 1 are small and in the range of their large uncertainty due to the overlap of two processes, peat 1 was also excluded, but will be discussed in a separate study (Kunhi Mouvenchery et al. 2013).

3.4 Effect of cation addition on cation content and DOC loss of OSL

Cation content In the Al- and in the Ca-treated OSL, cation content increased with increasing concentration of the salt solution and leveled out at a maximum (Fig. 3). The maximum Ca^{2+} content ranged between 270 and 300 $mmol_c kg^{-1}$ and was in the range of CEC_{eff}. Thus, all exchange sites accessible for Ca^{2+} were saturated with Ca^{2+}. The content of exchangeable Mg^{2+} decreased from 40 $mmol_c kg^{-1}$ (control) to almost 0 $mmol_c kg^{-1}$ with increasing concentrations of Ca^{2+}

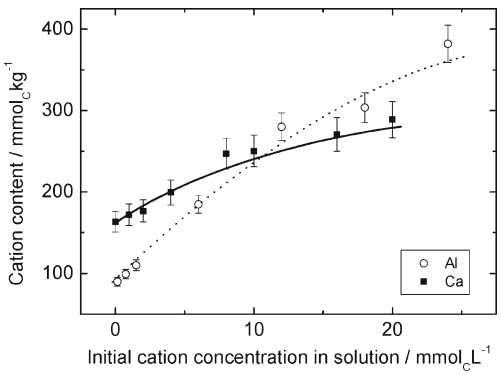

Fig. 3 Calcium content and aluminum content in OSL after batch experiments as function of initial cation concentrations in batch solution; *error bars* show standard errors calculated from three to seven measurements per sample. The *solid and the dotted lines* visualize the nonlinear dependency of the cation uptake on the initial solution concentration of calcium and aluminum, respectively

in the solution, which shows that Ca^{2+} mainly replaces Mg^{2+} from its exchange sites. This observation is in line with studies reporting preference of SOM for the sorption of Ca^{2+} over Mg^{2+} due to the strongly held hydration shell of Mg^{2+} and the tendency of Ca^{2+} to form inner sphere complexes (Kalinichev and Kirkpatrick 2007). Besides Mg^{2+}, some Mn^{2+} was replaced by Ca^{2+}, indicated by a decrease of the Mn^{2+} content from 10 to 4 $mmol_c kg^{-1}$. Na^+ preferentially replaced Ca^{2+} (decrease from 160 to 100 $mmol_c kg^{-1}$) and Mg^{2+} (decrease from 40 to 5- $mmol_c kg^{-1}$), but not Al^{3+} and Fe^{3+}. In total, 95 $mmol_c kg^{-1}$ of Ca^{2+} plus Mg^{2+} ions was exchanged by Na^+. Al^{3+} and Fe^{3+} contents remained unchanged irrespective the concentration of Ca^{2+} and Na^+ in treatment solutions (data not shown).

In contrast, Al^{3+} uptake even exceeded CEC_{eff} for high Al concentrations. Inorganic Al precipitates are expected to be negligible below pH 4 (Johnson 2002; Nierop et al. 2002), but organic DOM-Al precipitates may have been formed or Al^{3+} might have exchanged cations not exchangeable with Ba^{2+}. This assumption is supported by the exchange with Fe^{3+} observed only for the Al-treated samples, underlining the larger exchange capability of Al^{3+} than of any bivalent cation. Alternatively, single cation exchange sites without neighbors in sufficiently close proximity may be occupied by Al^{3+} accompanied by counterions. Furthermore, competition for exchange sites may additionally lead to occupation of formerly cross-linked exchange sites by two individual cations and therefore to a disruption of cross-links.

Loss of dissolved organic carbon All treated samples exhibited considerably smaller DOC concentrations in the supernatant (1.5±0.2 mg kg^{-1}) than the control samples (2.0±0.1 mg kg^{-1}). DOC concentration tended to decrease with increasing initial cation concentration with slopes of −0.019 mg DOC $(mmol_c)^{-1}$ for Al^{3+} and -0.012 mg DOC $(mmol_c)^{-1}$ for Ca^{2+}. Although not significant ($P \geq 0.1$), this trend cannot be disregarded and is in line with other studies (Römkens and Dolfing 1998; Schaumann 2000). The strong efficiency of Al^{3+} to reduce DOC and thus to bind DOC fits well to the observation that Al^{3+} can decrease mineralization of DOC to up to 50% (Schwesig et al. 2003). In this view, the Al^{3+} contents in the OSL above CEC_{eff} could also be due to precipitation or flocculation of additional DOM from the treatment solution, resulting in a significant amount of Al–OM associates. In the Ca treatment, this DOM remained in the liquid phase.

3.5 Effect of cation addition on *T**

After 4 weeks of storage, all controls revealed an average *T** of 57.8±0.4 °C. *T** of the Na-treated samples averaged at 59.2±0.6 °C independently of Na content. Ca and Al treatment resulted in *T** of up to 60.0 and 61.6 °C, respectively. All *T** values were in the range of *T** normally found for organic soil samples (Hurrass and Schaumann 2005). The standard error of *T** averaged 0.4 °C for the Al-treated samples and resembled that for other studies (Hurrass and Schaumann 2005). Ca-treated samples and Na-treated samples revealed larger standard errors (0.6–0.7 °C), which suggests higher heterogeneity of the matrix. *T** of the Ca-treated samples and the Al-treated samples increased with increasing cation content (Fig. 4). This trend was significant for cation loadings up to 200 $mmol_c kg^{-1}$ ($P<0.05$). Higher cation contents did not further increase *T** significantly.

In order to compare the effects of all cation treatments although different in concentration dependence, we subdivided the data of the Ca-treated and Al-treated OSL into two groups: Concentration range 1 ("low") refers to cation loadings below 200 $mmol_c kg^{-1}$, and concentration range 2 ("high") refers to cation loadings above 200 $mmol_c kg^{-1}$. The resulting datasets are shown in box plots in Fig. 5a. Average *T** was lowest in the demineralized sample (56.7 °C), followed by the control (57.8 °C), the Na- and Ca-treated samples (58.6–59.2 °C), and the Al-treated samples (low, 59.5 °C; high, 61.4 °C). Except for the Na-treated samples, most differences between the different treatments were significant (see Fig. 5a).

Figure 5b shows the cation effects on *T**, calculated as difference between average *T** of the treatment and that of the control. Demineralization significantly reduced *T** by 1.1 °C, Na and Ca treatment resulted in a comparable increase of *T** (increase of 0.8–1.5 °C), and Al treatment caused the strongest increase in *T** (1.7–3.6 °C), especially for Al loadings above 200 $mmol_c kg^{-1}$.

These results demonstrate that (a) *T** increases with cation loading for loadings below CEC_{eff}, (b) no further increase in *T** occurs when the cation loading reaches CEC_{eff}, although cation loading can exceed CEC_{eff}, and (c) Al treatment results in a more homogeneous matrix than Ca^{2+} and Na^+ treatment. In the light of the hypothesized CaB, this implies that cation

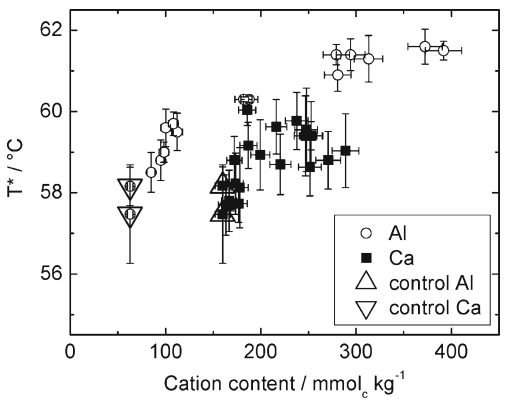

Fig. 4 WaMB transition temperature *T** in dependence of calcium content and aluminum content in OSL after 4 weeks of storage at 20 °C and 76% relative humidity; *error bars* show standard errors calculated from three to seven measurements per sample. The *triangles* mark the data of the controls

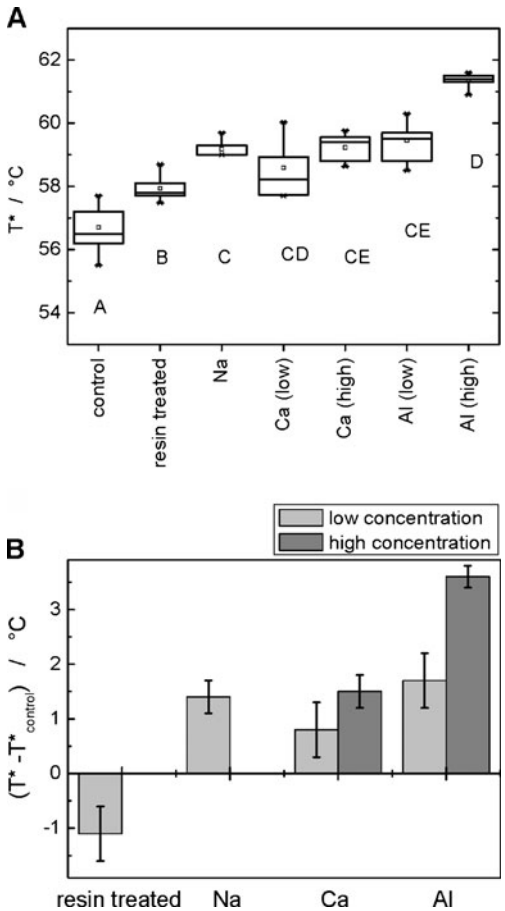

Fig. 5 **a** Box plots of the variation of WaMB transition temperatures, *T**, for all cation treatments of OSL: *resin treated* samples demineralized with cation exchange resin; *control* control samples; *Na*, *Ca*, *Al* samples treated with Na, Ca, and Al, respectively. Differentiation between low and high concentration range for Ca and Al: *low* cation loading below 200 $mmol_c kg^{-1}$; *high* above 200 $mmol_c kg^{-1}$. The *letters below the box plots* indicate the affiliation to different groups differing significantly from each other ($P<0.05$). The dataset of the control sample differs significantly from those of all other samples. **b** Cation effect on *T**: difference between the average *T** of the cation-treated samples and that of the control. Concentration range 1 refers to all controls, resin-treated samples, and Na samples, as well as to Ca- and Al-treated samples with cation loadings below 200 $mmol_c kg^{-1}$. Concentration range 2 addresses Ca- and Al-treated samples with cation loadings above 200 $mmol_c kg^{-1}$

addition increases the amount of CaB for low cation loadings. This effect increases with increasing cation loading and valency and is in line with the reduction of molecular mobility by Ca and Al observed with NMR for a HA (Nebbioso and Piccolo 2009). At higher loadings, cation addition can result in the reverse effect: CaB can be disrupted due to competition of numerous cations for exchange sites. This may oversaturate the exchanger and additionally bind anions into the matrix to maintain charge neutrality. In this situation, *T** remains unaffected or even decreases with increasing cation saturation.

Up to this point, our data largely support the idea of direct CaB effective in the solid, air-dried organic matter, with a stiffening effect increasing with cation loading and valency. However, the higher heterogeneity of Na- and Ca-treated samples than of Al-treated samples needs further explanation. Al^{3+} can be more selective for certain cross-linking sites and immediately form inner sphere complexes with OM. For Ca^{2+} and Na^{+}, the balance between energy gain due to formation of inner sphere complexes and energy required to release the hydration shell is not that clearly pronounced. Therefore, a larger variety of complexes is expected in the beginning, especially during cation treatment, ranging from outer sphere complexes (Aquino et al. 2011) to stable inner sphere complexes (Kalinichev and Kirkpatrick 2007) before aging and drying successively increases the percentage of inner sphere complexes and the relevance of short-range interactions.

3.6 Effect of aging on *T**

To obtain further evidence for or against the classical cross-linking hypothesis, we investigated aging effects on *T** of the solid OSL. Assuming direct CaB, aging should overcome initial sample heterogeneity and increase both *T** and valency- and concentration-dependent differences in *T**.

Sample storage resulted in a significant increase of *T** for all samples compared to the nonaged samples ($P<0.05$, Fig. 6). *T** reached values of 60.5 °C for the control, 60.0 °C for the Na-treated OSL, 61.1–61.4 °C for the Ca-treated OSL and the Al-treated OSL (low), and 62.0 °C for Al-treated sample (high; see Fig. 6a). The standard error of *T** after aging was 0.4 °C for all treatments, indicating homogenization of Na- and Ca-treated OSL. However, differences between the treatments decreased upon aging: Only for the aged Na-treated OSL and Al-treated OSL above 200 $mmol_c kg^{-1}$, *T** still differed significantly from that of the aged control ($T^*_{Na}-T^*_{control}=-0.5$ °C and $T^*_{Al}-T^*_{control}=+1.5$ °C), indicating a flexibilization by Na and stiffening by Al in the aged sample. It cannot be excluded that initially observed cation and concentration dependence are successively canceled out with aging.

The aging effect on *T** ($T^*_{i,\,aged}-T^*_{i,\,nonaged}$) ranged between +0.6 and +2.7 °C and was strongest for the control and for Ca treatment (see Fig. 6b). It was significantly smaller for Ca- and Al-treated samples with high cation loading (1.8 and 0.6 °C, respectively) than for low cation loadings (2.5 and 0.9 °C, respectively). It further increased with decreasing initial *T** ($P=0.05$; see Fig. 6c). Thus, initially least stable WaMB have the strongest aging effect.

Thus, some observations support classical cross-linking: *T** increased upon aging, aged samples were more homogeneous, Na destabilized the aged matrix; and Al stabilized it. However, the differences between sample treatments decreased with aging time and the aging effect increased with decreasing initial *T**. These observations contradict the classical cross-linking hypothesis.

The convergence of *T** suggests that the aging process is due to a similar mechanism in all samples, independently of the

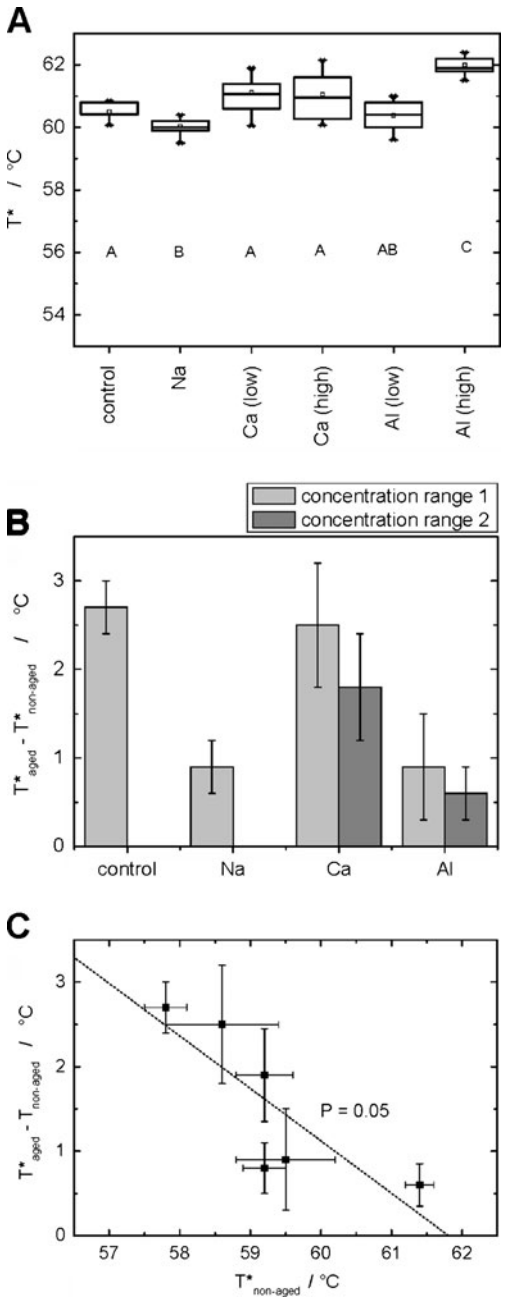

Fig. 6 **a** WaMB transition temperature, *T**, after aging of at least 8 weeks for the control and the Na-, Ca-, and Al-treated samples, respectively. **b** Aging effect on *T** for the different treatments. Concentration ranges 1 and 2 match with those described in the caption of Fig. 5. **c** Aging effect in dependence of the initial *T** before aging for all sample sets. The *x*- and *y-error bars* correspond to the standard deviation within each sample set

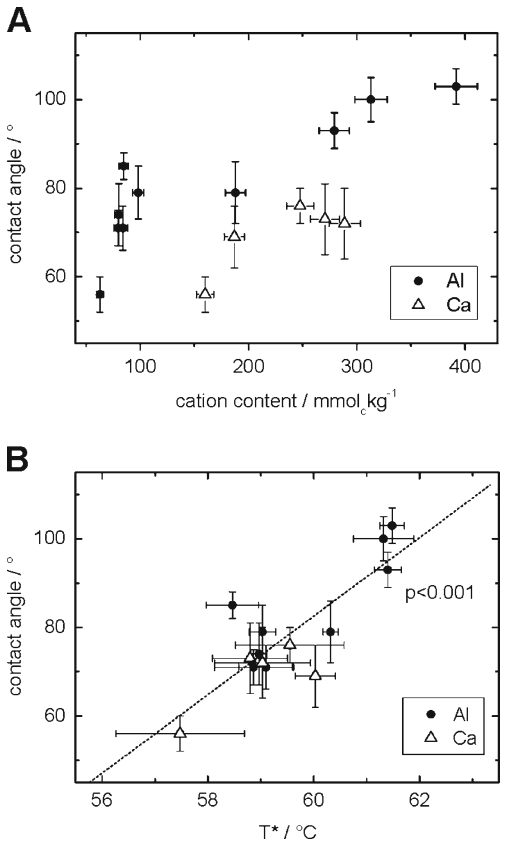

Fig. 7 **a** Contact angle of the Ca- and Al-treated samples after 4 weeks of storage at 20 °C and 76% relative humidity in dependency of cation content. **b** Relation between the step transition temperature, *T**, of all treatments and CA. The *dashed line* indicates the relation between CA and *T** (complete dataset of all treated and untreated samples). Please note that each data point is the average of all sample and measurement repetitions. *Error bars* in **a** and **b** show standard errors calculated from three to seven measurements per sample

cation. We assume that aging involves redistribution of water molecules leading to a successively increasing number and strength of WaMB (Schaumann and Bertmer 2008; Schaumann 2005). The decrease in the relevance of cation type and concentration with aging time suggests that the resulting supramolecular network in the OM is dominated by WaMB interacting with cations. The explanation that direct Al CaB form faster and more selectively than Ca CaB implies that further aging processes would be less effective for Al bridges because the favorable sites had already been occupied in the beginning. This is in line with the small aging effect in Al-treated samples.

If predominantly the WaMB network determines matrix rigidity, this would also explain the observation that aged Ca-treated samples exhibit *T** values comparable to that of aged Al-treated samples and that heterogeneity of Ca-treated samples decreases with storage. During aging, redistribution of weakly bound Ca^{2+} ions and water molecules could increase the degree and strength of cross-linkage. Moreover, the cations can successively occupy sites which had been linked by water molecule bridges before cation treatment, and could undergo CaB associated with WaMB (Schaumann et al. 2013).

3.7 Effect of cation addition on contact angle

The CA of treated and untreated samples behaved in similar manner as *T**. It increased with increasing Ca^{2+} and Al^{3+} content of the sample below 200 $mmol_c kg^{-1}$, flattened for higher Al^{3+} contents, and even decreased again for Ca-treated samples

(Fig. 7a). As for T^*, Al treatment was more effective than Ca treatment. Combining all CA data resulted in a clear linear correlation between CA and T^* ($P<0.001$; see Fig. 7b), although data points are grouped in three regions. This indicates that rigidity of the OM matrix is closely linked to wettability. Diehl and Schaumann (2007) identified a physical and chemical process responsible for changes in hydrophobicity of soil samples. The chemical process involves reorientation of hydrophilic OM groups on the surface towards the SOM interior where they are fixed by H bonds or ester linkages, resulting in higher surface hydrophobicity. In the same way, it can be assumed that cations fix functional groups and block their reorientation towards the outer surface.

4 Conclusions

Our results support the idea that multivalent cations form CaB and increase matrix rigidity in solid soil organic matter. However, only the short-term effects (4 weeks) are in line with the currently accepted classical cross-linking hypothesis. The convergence of T^* upon aging for most cations and concentrations and the increase in aging effect with decreasing valency point to the relevance of WaMB interacting with CaB and increasing in strength. CaB–WaMB associations have been suggested only recently from NMR investigations of a peat (Schaumann et al. 2013). Considering that matrix rigidity acts as kinetic barrier for diffusion of ions and molecules, CaB and WaMB directly control kinetic availability of nutrients and organic chemicals in soil. As they are subjected to continuous dynamics, release of ions and molecules from soils will be slower under constant environmental conditions than after changes in cation or moisture status.

A second important outcome of this study is the observation that not only drying (Doerr et al. 2007), but also CaB alter hydrophobicity soils. Both effects arise from reorientation of hydrophilic functional OM groups towards the interior. CaB in the interior will block reorientation of functional groups towards the surface, with the consequence of higher wetting resistance and persistence of water repellency than due to sole drying-induced reorientation mechanisms.

Still, the transferability of the results of this study to other soils needs to be tested. The sample-dependent reaction of the WaMB transition temperature on cation removal suggests that other soils may give apparently conflictive results. The results of the cation addition study of peat 1 (Kunhi Mouvenchery et al. 2013) even suggest low relevance of CaB. This and our current findings suggest that the main difference in reaction of WaMB stability on cation treatment is determined by cation exchange capacity, which determines the amount and distances of potential cross-linking sites and the current cation loading of the sample. The knowledge of this interplay is highly relevant for the mechanistic understanding of functioning of biogeochemical interfaces under environmental conditions in the field.

Acknowledgments We acknowledge the financial support of the CROSSLINK project and the priority program SPP 1315 by the German Research Foundation (DFG, SCHA 849/6, and SCHA 849/8). Furthermore, we thank Susanne Woche and Jörg Bachmann for sampling of peat 1, Friederike Lang for providing the OSL sample, as well as for many helpful discussions, Sören Thiele-Bruhn and Tatjana Schneckenburger for providing the peat 2 sample and analyzing the Al samples, and Sabina Hens for her help in the laboratory.

References

Aquino AJA, Tunega D, Schaumann GE, Haberhauer G, Gerzabek MH, Lischka H (2009) Stabilizing capacity of water bridges in nanopore segments of humic substances: a theoretical investigation. J Phys Chem C 113:16468–16475

Aquino AJA, Tunega D, Schaumann GE, Haberhauer G, Gerzabek MH, Lischka H (2011) The functionality of cation bridges for binding polar groups in soil aggregates. Int J Quantum Chem 111:1531–1542

Diehl D, Schaumann GE (2007) The nature of wetting on urban soil samples: wetting kinetics and evaporation assessed from sessile drop shape. Hydrol Process 21(17):2255–2265

Diehl D, Bayer JV, Woche SK, Bryant R, Doerr SH, Schaumann GE (2010) Reaction of soil water repellency on artificially induced changes in soil pH. Geoderma 158(3–4):375–384

Doerr SH, Shakesby SH, Walsh RPD (2000) Soil water repellency: its causes, characteristics and hydro-geomorphological significance. Earth Sci Rev 51(1–4):33–65

Doerr SH, Ritsema CJ, Dekker LW, Scott DF, Carter D (2007) Water repellence of soils: new insights and emerging research needs. Hydrol Process 21(17):2223–2228

Gaiffe M, Duquet B, Tavant H, Tavant Y, Bruckert S (1984) Biological stability and physical behavior of an argillohumic complex placed under different conditions of saturation with calcium or potassium. Plant Soil 77(2–3):271–284

Gustafsson JP, Pechova P, Berggren D (2003) Modeling metal binding to soils: the role of natural organic matter. Environ Sci Technol 37(12):2767–2774

Hurrass J, Schaumann GE (2005) Is glassiness a common characteristic of soil organic matter? Environ Sci Technol 39(24):9534–9540

Hurraß J, Schaumann GE (2007) Influence of the sample history and the moisture status on the thermal behavior of soil organic matter. Geochim Cosmochim Acta 71:691–702

Jaeger F, Shchegolikhina A, van As H, Schaumann GE (2010) Proton NMR relaxometry as a useful tool to evaluate swelling processes in peat soils. Open Magn Reson J 3:27–45

Jaeger A, Schaumann GE, Bertmer M (2011) Optimized NMR spectroscopic strategy to characterize water dynamics in soil samples. Org Geochem 42(8):917–925

Johnson CE (2002) Cation exchange properties of acid forest soils of the northeastern USA. Eur J Soil Sci 53(2):271–282

Kalinichev AG, Kirkpatrick RJ (2007) Molecular dynamics simulation of cationic complexation with natural organic matter. Eur J Soil Sci 58(4):909–917

Kaupenjohann M, Wilcke W (1995) Heavy-metal release from a serpentine soil using a Ph-stat technique. Soil Sci Soc Am J 59(4):1027–1031

Kunhi Mouvenchery Y, Kučerík J, Diehl D, Schaumann GE (2012) Cation-mediated cross-linking in natural organic matter—a

review. Rev Environ Sci Biotechnol 11(1):41–54. doi:10.1007/s11157-011-9258-3

Kunhi Mouvenchery Y, Jaeger A, Aquino AJA, Tunega D, Diehl D, Bertmer M, Schauman GE (2013) Restructuring of a peat in interaction with multivalent cations: effect of cation type and aging time. PlosOne 8(6):e65359. doi:10.1371/journal.pone.0065359

Lang F, Kaupenjohann M (2004) Trace element release from forest floor can be monitored by ion exchange resin tubes. J Plant Nutr Soil Sci 167:177–183

LeBoeuf EJ, Weber WJ Jr (2000a) Macromolecular characteristics of natural organic matter. 2. Sorption and desorption behavior. Environ Sci Technol 34(17):3632–3640

LeBoeuf EJ, Weber WJ (2000b) Macromolecular characteristics of natural organic matter. 1. Insights from glass transition and enthalpic relaxation behavior. Environ Sci Technol 34(17):3623–3631

Lewis AL, Miller JD (1993) Coordinative crosslinking of pyridyl- and bipyridyl-based hydrogel polymer membranes. Polymer 34(11):2453–2457

Li Y, Tan W, Koopal LK, Wang M, Liu F, Norde W (2013) Influence of soil humic and fulvic acid on the activity and stability of lysozyme and urease. Environ Sci Technol 47(10):5050–5056

Lu Y, Pignatello JJ (2004) Sorption of apolar aromatic compounds to soil humic acid particles affected by aluminum(III) ion cross-linking. J Environ Qual 33(4):1314–1321

Nebbioso A, Piccolo A (2009) Molecular rigidity and diffusivity of Al3+ and Ca2+ humates as revealed by NMR spectroscopy. Environ Sci Technol 43(7):2417–2424

Nierop KGJ, Jansen B, Verstraten JA (2002) Dissolved organic matter, aluminium and iron interactions: precipitation induced by metal/carbon ratio, pH and competition. Sci Total Environ 300(1–3):201–211

Piccolo A (2002) The supramolecular structure of humic substances: a novel understanding of humus chemistry and implications in soil science. Adv Agron 75:57–134

Pignatello JJ (2012) Dynamic interactions of natural organic matter and organic compounds. J Soils Sediments 12(8):1241–1256

Römkens P, Dolfing J (1998) Effect of Ca on the solubility and molecular size distribution of DOC and Cu binding in soil solution samples. Environ Sci Technol 32:363–369

Schaumann GE (2000) Effect of CaCl2 on the kinetics of the release of dissolved organic matter (DOM). J Plant Nutr Soil Sci 163(5):523–529

Schaumann GE (2005) Matrix relaxation and change of water state during hydration of peat. Colloid Surf A 265(1–3):163–170

Schaumann GE (2006) Soil organic matter beyond molecular structure. 2. Amorphous nature and physical aging. J Plant Nutr Soil Sci 169(2):157–167

Schaumann GE, Bertmer M (2008) Do water molecules bridge soil organic matter molecule segments? Eur J Soil Sci 59(3):423–429

Schaumann GE, LeBoeuf EJ (2005) Glass transitions in peat—their relevance and the impact of water. Environ Sci Technol 39(3):800–806

Schaumann GE, Thiele-Bruhn S (2011) Molecular modelling of soil organic matter: squaring the circle? Geoderma 169:55–68

Schaumann GE, Siewert C, Marschner B (2000) Kinetics of the release of dissolved organic matter (DOM) from air-dried and pre-moistened soil material. J Plant Nutr Soil Sci 163(1):1–5

Schaumann GE, LeBoeuf EJ, DeLapp RC, Hurraß J (2005) Thermomechanical analysis of air-dried whole soil samples. Thermochim Acta 436(1–2):83–89

Schaumann GE, Diehl D, Bertmer M, Jaeger A, Conte P, Alonzo G, Bachmann J (2013) Combined proton NMR wideline and NMR relaxometry to study SOM-water interactions of cation-treated soils. J Hydrol Hydromech 61:50–63

Scheel T, Jansen B, van Wijk AJ, Verstraten JM, Kalbitz K (2008) Stabilization of dissolved organic matter by aluminium: a toxic effect or stabilization through precipitation? Eur J Soil Sci 59(6):1122–1132

Schneckenburger T, Schaumann GE, Woche SK, Thiele-Bruhn S (2012) Short-term evolution of hydration effects on soil organic matter properties and resulting implications for sorption of naphthalene-2-ol. J Soils Sediments 12(8):1269–1279

Schwesig D, Kalbitz K, Matzner E (2003) Effects of aluminium on the mineralization of dissolved organic carbon derived from forest floors. Eur J Soil Sci 54(2):311–322

Seyler RJ (ed) (1994) Assignment of the glass transition, vol 1249. American Society for Testing and Materials, Philadelphia

Simpson AJ, Kingery WL, Hayes MHB, Spraul M, Humpfer E, Dvortsak P, Kerssebaum R, Godejohann M, Hofmann M (2002) Molecular structures and associations of humic substances in the terrestrial environment. Naturwissenschaften 89(2):84–88

Suvorova AI, Tjukova IS, Trufanova EI (1999) Thermodynamic and diffusion properties of biodegradable systems based on starch and cellulose derivatives. J Environ Polym Degr 7(1):35–40

Tan WF, Koopal LK, Norde W (2009) Interaction between humic acid and lysozyme, studied by dynamic light scattering and isothermal titration calorimetry. Environ Sci Technol 43(3):591–596

Tan W-F, Norde W, Koopal LK (2011) Humic substance charge determination by titration with a flexible cationic polyelectrolyte. Geochim Cosmochim Acta 75(19):5749–5761

Virto I, Moni C, Swanston C, Chenu C (2011) Turnover of intra- and extra-aggregate organic matter at the silt-size scale. Geoderma 156(1–2):1–10

Wershaw RL (2004) Evaluation of conceptual models of natural organic matter (humus) from a consideration of the chemical and biochemical processes of humification scientific investigations report 2004–5121. U.S. Department of the Interior, U.S. Geological Survey Reston, Virginia

Yang Y, Ratte D, Smets BF, Pignatello JJ, Grasso D (2001) Mobilization of soil organic matter by complexing agents and implications for polycyclic aromatic hydrocarbon desorption. Chemosphere 43(8):1013–1021

Yuan G, Xing B (2001) Effects of metal cations on sorption and desorption of organic compounds in humic acids. Soil Sci 166(2):107–115